Molecular Cell

Article

Replication Stress Induces ATR/CHK1-Dependent Nonrandom Segregation of Damaged Chromosomes

Graphical Abstract

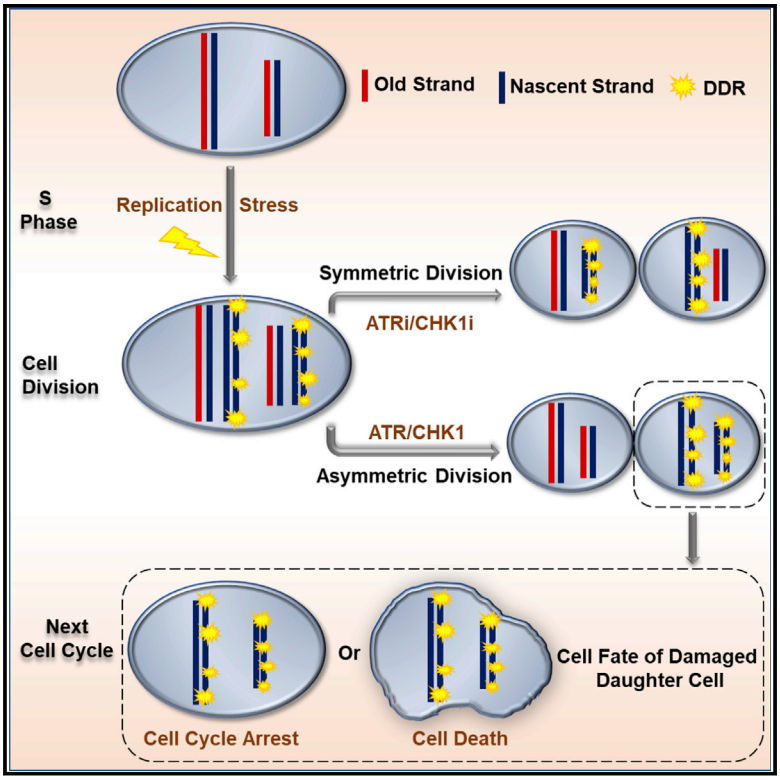

Highlights

- Replication stress induces nonrandom chromatid segregation
- Replication stress induces asymmetric distribution of DNA damage response proteins
- Nonrandom DNA segregation is dependent on ATR/CHK1 activity
- Asymmetric division induces genomic instability or cell death in damaged daughter cells

Authors

Meichun Xing, Fengjiao Zhang, Hongwei Liao, ..., Ian D. Hickson, Huahao Shen, Songmin Ying

Correspondence

yings@zju.edu.cn (S.Y.), huahaoshen@zju.edu.cn (H.S.), iandh@sund.ku.dk (I.D.H.)

In Brief

Xing et al. show that nonrandom chromatid segregation, together with the asymmetric DNA damage response, is induced by replication stress, which ultimately leads to genomic instability and cell death in damaged daughter cells.

Xing et al., 2020, Molecular Cell *78*, 1–11
May 21, 2020
https://doi.org/10.1016/j.molcel.2020.04.005

CellPress

Please cite this article in press as: Xing et al., Replication Stress Induces ATR/CHK1-Dependent Nonrandom Segregation of Damaged Chromosomes, Molecular Cell (2020), https://doi.org/10.1016/j.molcel.2020.04.005

Molecular Cell

CellPress

Article

Replication Stress Induces ATR/CHK1-Dependent Nonrandom Segregation of Damaged Chromosomes

Meichun Xing,[1,5] Fengjiao Zhang,[1,5] Hongwei Liao,[1] Sisi Chen,[1] Luanqing Che,[2] Xiaohui Wang,[1] Zhengqiang Bao,[1] Fang Ji,[1] Gaoying Chen,[1] Huihui Zhang,[1] Wen Li,[2] Zhihua Chen,[2] Ying Liu,[3] Ian D. Hickson,[3,*] Huahao Shen,[2,4,*] and Songmin Ying[1,6,*]

[1]Department of Pharmacology and Department of Respiratory and Critical Care Medicine of the Second Affiliated Hospital, Zhejiang University School of Medicine, Key Laboratory of Respiratory Disease of Zhejiang Province, Hangzhou 310009, China

[2]Key Laboratory of Respiratory Disease of Zhejiang Province, Department of Respiratory and Critical Care Medicine, Second Affiliated Hospital of Zhejiang University School of Medicine, Hangzhou, Zhejiang 310009, China

[3]Center for Chromosome Stability and Center for Healthy Aging, Department of Cellular and Molecular Medicine, University of Copenhagen, Blegdamsvej 3B, 2200 Copenhagen N, Denmark

[4]State Key Laboratory of Respiratory Diseases, Guangzhou, Guangdong 510120, China

[5]These authors contributed equally

[6]Lead Contact

*Correspondence: yings@zju.edu.cn (S.Y.), huahaoshen@zju.edu.cn (H.S.), iandh@sund.ku.dk (I.D.H.)

https://doi.org/10.1016/j.molcel.2020.04.005

SUMMARY

Nonrandom DNA segregation (NDS) is a mitotic event in which sister chromatids carrying the oldest DNA strands are inherited exclusively by one of the two daughter cells. Although this phenomenon has been observed across various organisms, the mechanism and physiological relevance of this event remain poorly defined. Here, we demonstrate that DNA replication stress can trigger NDS in human cells. This biased inheritance of old template DNA is associated with the asymmetric DNA damage response (DDR), which derives at least in part from telomeric DNA. Mechanistically, we reveal that the ATR/CHK1 signaling pathway plays an essential role in mediating NDS. We show that this biased segregation process leads to cell-cycle arrest and cell death in damaged daughter cells inheriting newly replicated DNA. These data therefore identify a key role for NDS in the maintenance of genomic integrity within cancer cell populations undergoing replication stress due to oncogene activation.

INTRODUCTION

It is generally considered that the distribution of cell constituents between the two daughter cells during cell division is equal. However, this dogma has been challenged recently by evidence indicating that asymmetric cell division is fundamental in many aspects of stem cell biology (Habib et al., 2013; Rocheteau et al., 2012; Tran et al., 2012; Zimdahl et al., 2014), in lymphocytes (Chang et al., 2011; Thaunat et al., 2012; Verbist et al., 2016), and in cancer (Knoblich, 2010; Zhang et al., 2014). The phenomenon of asymmetric cell division has been widely discussed in the context of nonnuclear components and nuclear components in different organisms (Burke, 2013; Denoth-Lippuner et al., 2014; Derivery et al., 2015; Gallo et al., 2010; Katajisto et al., 2015; Kressmann et al., 2015; Liu et al., 2013; Lopez-Vernaza and Leach, 2013; Yang et al., 2015). There has been a long-standing interest in the possibility that chromosomes segregate nonrandomly during mitosis and that some of the differences between mother and daughter cells could be explained by selective chromatid segregation. However, the mechanism underlying nonrandom separation of sister chromatids has remained elusive (Akera et al., 2017; Ginda et al., 2017; Yadlapalli and Yamashita, 2013), despite the so-called immortal strand hypothesis (Cairns, 1975), which was put forward decades ago as a potential explanation for how long-lived daughter stem cells might retain genomic integrity. The validity of the immortal strand hypothesis is still controversial, and it is not clear why some cells might retain their template DNA and whether or not the phenomenon is restricted to stem cells (Lansdorp, 2007; Rando, 2007).

Nonrandom DNA segregation (NDS) has been observed in stem cells, fibroblasts, and epithelial, neural, and muscle satellite cells (Conboy et al., 2007; Freida et al., 2013; Karpowicz et al., 2005; Potten et al., 1978; Rebollo et al., 2007; Shinin et al., 2006). Several studies have demonstrated that epidermal basal cells, hematopoietic stem cells, and intestinal epithelial stem cells segregate their chromosomes randomly (Barker et al., 2007; Charville and Rando, 2011; Escobar et al., 2011; Kiel et al., 2007; Sotiropoulou et al., 2008; Zimdahl et al., 2014). Certain cancer cell lines harbor a subpopulation of cells exhibiting NDS, which is modulated by stress conditions such as high cell density, hypoxia, and serum deprivation (Pine et al., 2010), suggesting that stress signaling from the microenvironment

Please cite this article in press as: Xing et al., Replication Stress Induces ATR/CHK1-Dependent Nonrandom Segregation of Damaged Chromosomes, Molecular Cell (2020), https://doi.org/10.1016/j.molcel.2020.04.005

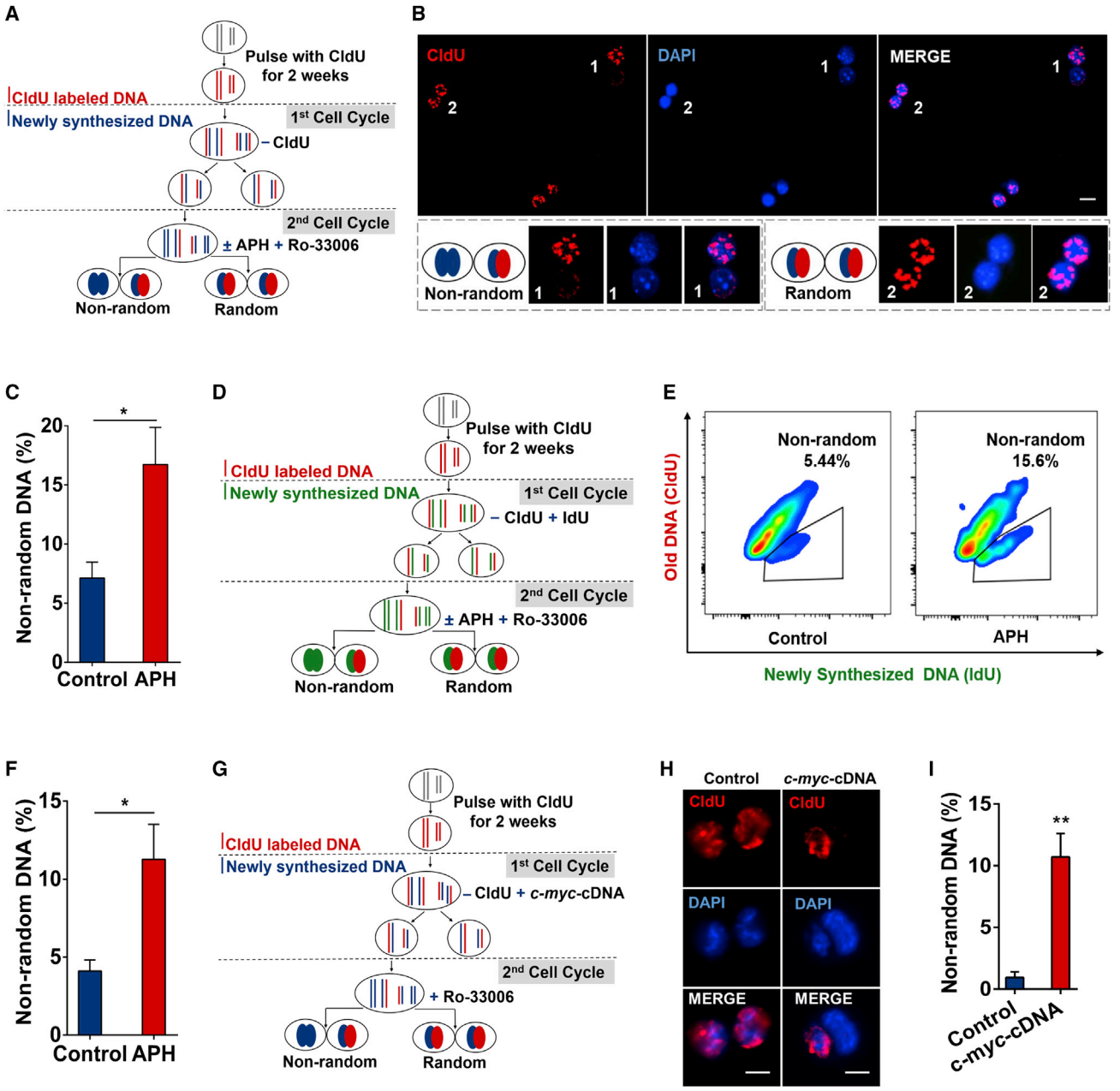

Figure 1. Replication Stress Induces Nonrandom Chromatid Segregation

(A) Schematic representation of random and nonrandom division of template DNA strands. Cells were grown in CldU (red) for 2 weeks to ensure that all parental DNA was labeled. CldU was then removed and the cells were allowed to progress through one cell cycle in CldU-free medium. During the second cell division following removal of CldU (the chase), cells were synchronized using RO-3306 in late G2 and then released into mitosis. The sister chromatids containing the CldU-labeled template DNA were then segregated either randomly or exclusively to one of the two daughter cells.

(B) Representative images of daughter cells that partition their CldU-labeled template DNA (red) either randomly (Crop image 2) to both daughter cells or exclusively to the one daughter cell (Crop image 1). Scale bars, 10 μm.

(C) Quantification of the frequency of NDS in U2OS cells without (n = 452) or with (n = 396) APH treatment.

(D) Schematic representation of random and nonrandom division of template DNA. Cells were grown in CldU (red). During the second cell division following removal of CldU, IdU (green) was added, and the IdU-labeled new DNA strands were then segregated either randomly (random) or exclusively to one of the daughter cells (nonrandom).

(E and F) U2OS daughter cells in G1 (cyclin A negative) were gated and sorted into CldU-positive and IdU-positive fractions and then analyzed for the percentage of nonrandom segregation (only IdU-labeled DNA) by flow cytometry. (E) Representative FACS images of control and APH-treated cells. (F) Quantification of the data from (E.) At least 50,000 cells were analyzed in each condition.

(legend continued on next page)

Please cite this article in press as: Xing et al., Replication Stress Induces ATR/CHK1-Dependent Nonrandom Segregation of Damaged Chromosomes, Molecular Cell (2020), https://doi.org/10.1016/j.molcel.2020.04.005

plays an important role in NDS. One potentially relevant feature of cancers is their propensity to develop so called DNA replication stress, which is largely linked to a deregulation of the cell cycle resulting from the activation of oncogenes during tumorigenesis. Replication stress is a perturbation of DNA replication that causes DNA replication forks to progress slowly or stall. In this study, we set out to investigate whether replication stress might be a factor that could trigger NDS in mitosis and, furthermore, whether this process could be modulated and linked to cell fate.

RESULTS

Replication Stress Induces Nonrandom Chromatid Segregation in Human Cells

Using a pulse-chase experiment (Escobar et al., 2011; Pine et al., 2010; Shinin et al., 2006) (Figure 1A), we observed that the older parental DNA strands (labeled with a DNA analog, chlorodeoxyuridine [CldU]) of most or all sister chromatids were nonrandomly segregated in mitosis in the human U-2OS osteosarcoma cell line in a small proportion of the cell population (~7%) (Figures 1B, 1C, S1A, and S1B). To address the possibility that this might be triggered by replication stress, we treated several cell lines, including cancer-derived U-2OS, A549, HCT116, and HeLa, and the primary cell line HFF-1 (human foreskin fibroblast) (Gravel et al., 2017; Morales et al., 1999; Schnabl et al., 2002), with the DNA polymerase $\alpha/\delta/\varepsilon$ inhibitor aphidicolin (APH) at a low dose that slows, but does not arrest, S-phase progression. This regimen is used commonly to induce mild replication stress, which leads to incomplete DNA synthesis in the nascent DNA strands and replication slowing/stalling in some already difficult-to-replicate regions (Chan et al., 2009). We observed that APH treatment induced an elevated frequency of NDS compared to that in untreated cells, consistent with replication stress being a driver of NDS (Figures 1C and S2). To provide more direct evidence to support this conclusion, we analyzed cells in which newly synthesized DNA and the older template DNA strands could be distinguished from each other due to being labeled with IdU (iododeoxyuridine) and CldU, respectively (Figure 1D). Using a fluorescence-activated cell sorting (FACS)-based assay, we observed that exposure of cells to APH induced an elevated level of NDS (Figures 1E and 1F). To investigate whether non-cancer cells expressing an activated oncogene might also exhibit NDS, we created a derivative of mouse embryonic fibroblasts (MEFs) that overexpresses oncogenic c-Myc. Although the parental MEF cells displayed only a very low level of NDS, a substantial increase was observed following c-Myc overexpression (Figures 1G–1I and S1C). These data are consistent with the proposal that oncogene-induced replication stress induces the nonrandom segregation of parental and nascent DNA strands, at least in some cells in a population.

Replication Stress Induces Asymmetric Distribution of DDR Proteins

During replication stress, cells mobilize a network of DNA damage response (DDR) proteins in an attempt to resolve any DNA damage and subsequently to make cell fate decisions depending on the success or failure of DNA repair processes (Magdalou et al., 2014). Typically, these DDR factors form nuclear foci following DNA damage. We considered whether the distribution of replication-stress-induced DDR factors might also be biased between the daughter cells during NDS. To investigate this, we labeled the template DNA with CldU as described above and then simultaneously tracked the segregation of DDR foci and CldU-labeled DNA. We observed asymmetric segregation of foci for the single-stranded DNA-binding protein replication protein A (RPA) and the FANCD2 protein, which defines the location of common fragile sites and other loci that are particularly prone to replication-stress-induced DNA damage. More specifically, those daughter cells exhibiting DDR markers were generally CldU negative, indicating that they failed to receive the normal complement of parental DNA strands (Figure 2A). Moreover, there was a clear association between NDS and nonrandom DDR protein segregation. Indeed, in most cases where the DNA strands were partitioned nonrandomly, the RPA or FANCD2 foci were also asymmetrically distributed (Figures 2B and 2C). These data suggest that the asymmetric inheritance of DDR proteins (and by inference damaged DNA) might be the underlying mechanism for NDS.

Next, we sought more definitive evidence that replication stress induces asymmetric DDR protein segregation to daughter cells. To this end, we established a stable cell line ectopically expressing RPA protein tagged with mCherry. After exposing these cells to low-dose APH in S phase, we performed live-cell imaging and observed by that the fluorescent RPA protein segregated asymmetrically during cell division (Figure S3A). Furthermore, we also observed that the endogenous DDR protein FANCD2 was asymmetrically inherited by daughter cells, such that one daughter cell inherited most (or in some cases all) of the FANCD2 foci (Figures 3A, S4A, S4C, and S4E). Indeed, this asymmetric inheritance of endogenous DDR proteins was not limited to FANCD2, but endogenous RPA and γH2AX were also distributed asymmetrically following APH treatment (Figures 3B, S4B, S4D, S4F, and S4G). Quantification of these data indicated that mild replication stress in the form of a low dose of APH enhanced the frequency of asymmetric inheritance (using an asymmetry index; see Figure 3C legend) over 2-fold (Figure 3C). To analyze the generality of our findings, we studied two other classes of replication stress inducers, an inhibitor of the ATR kinase (ATRi) and a G-quadruplex DNA-stabilizing ligand (pyridostatin [PDS]). We observed that both the ATRi and PDS increased the frequency of asymmetric DDR protein segregation in daughter cells (Figure 3D). In contrast, although the radiomimetic agent bleomycin induced extensive DNA damage (Figure S3B), it did not produce any marked change in

(G) Schematic representation of a pulse chase experiment with c-Myc overexpression.
(H and I) Representative daughter cell images (H) and the quantification data (I) of MEF cells without (n = 610) or with (n = 455) c-Myc-induced replication stress. Scale bars, 10 μm.
Data are the mean ± SEM from three independent experiments. *p < 0.05, **p < 0.01, t test.

Please cite this article in press as: Xing et al., Replication Stress Induces ATR/CHK1-Dependent Nonrandom Segregation of Damaged Chromosomes, Molecular Cell (2020), https://doi.org/10.1016/j.molcel.2020.04.005

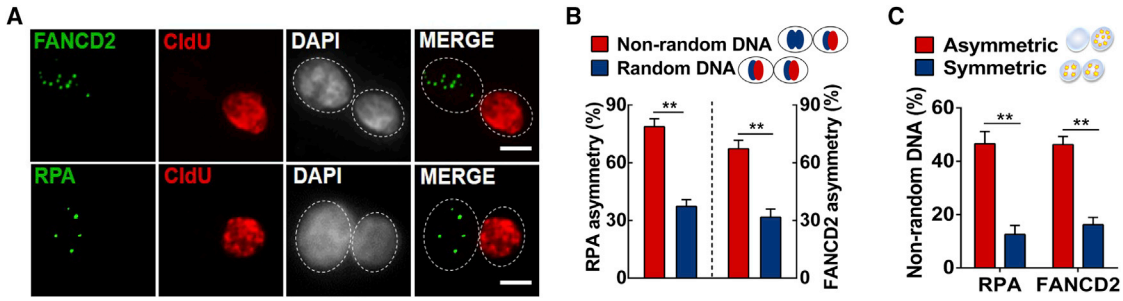

Figure 2. Daughter Cells with Immortal DNA Strands in NDS Contain Fewer DNA Damage Response (DDR) Foci

The cells were labeled and treated as described in Figure 1A.

(A–C) Images (A) and quantification (B and C) of co-stain CldU-labeled parental DNA and the FANCD2 (n = 354) and RPA (n = 476) proteins in daughter cells. Scale bars, 10 μm. Data are the mean ± SEM from three independent experiments. **p < 0.01, two-way ANOVA (B and C).

DDR protein segregation (Figure 3D). A similar result was observed for etoposide, a topoisomerase II inhibitor, where neither the symmetry of the DDR protein γH2AX nor NDS was affected (Figures S7C and S7D).

Thus far, our data indicate that DNA damage per se is not sufficient to activate NDS; instead, it appears that asymmetric DDR protein segregation is induced by various forms of replication stress. Consistent with this, we observed that primary MEF cells exhibited an increase in asymmetric γH2AX focus distribution in daughter cells following lentivirus-mediated expression of c-Myc (Figure 3E). Hence, oncogenic replication stress also induces asymmetric DDR protein segregation.

Telomeric Replication Stress Preferentially Induces Asymmetric DDR and NDS

To further explore the mechanism of asymmetric DDR distribution in detail, we analyzed the cellular response to PDS treatment, which is known to induce replication perturbation and fragility at telomeres (Min et al., 2017). PDS also promoted asymmetric DDR protein distribution in daughter cells, suggesting that telomeres might play a role in this process. To address this further, we analyzed the behavior of TRF2, which is a component of the telomere Shelterin protein complex. We observed that in those cases where the DDR protein γH2AX was segregated asymmetrically, TRF2 frequently co-localized with the γH2AX foci (Figure 4A). To eliminate the possibility that these TRF2 foci might form at non-telomeric loci, we analyzed telomeric DNA directly using a well-established cy3-$(TTAGGC)_3$ peptide nucleic acid (PNA) probe (5′). We demonstrated that this telomeric PNA probe also asymmetrically segregated together with the DDR protein FANCD2 (Figure 4B). Indeed, depletion of either TRF1 or TRF2 promoted asymmetric inheritance of DDR proteins under APH-induced replication stress (Figures 4C and S5A–S5E). As controls, we demonstrated that asymmetric FANCD2 foci rarely co-localized with rDNA loci (labeled by the UBF protein) or PML bodies (Figure S5F). Hence, we conclude that the asymmetric inheritance of DDR protein foci is frequently associated with telomeric DNA. Moreover, PDS induced a slightly higher rate of NDS in daughter cells than did APH (Figures 4D and 4E), suggesting that telomere dysfunction further aggravated NDS.

Replication Stress Induces ATR/CHK1-Dependent Asymmetric DDR and NDS

The ATR/CHK1 and ATM/CHK2 signaling pathways are important for the DDR and for telomere maintenance (Bartek et al., 2007; Bi et al., 2005). Therefore, we analyzed whether either of these signaling pathways might be activated in mitosis following replication stress. We observed that APH-induced replication stress elevated the level of CHK1 phosphorylation in mitotic cells (Figures 5A and S7A). Moreover, foci of phosphorylated CHK1 showed a strong degree of co-localization with the DDR protein RPA and the telomere-associated protein TRF2 (Figure 5B), suggesting that the ATR/CHK1 pathway might be important for the asymmetric DDR distribution. To investigate this further, we exposed cells to low-dose APH, synchronized them at the G2/M boundary, and then released into mitosis in the presence of an ATR, an ATM, or a CHK1 inhibitor (Figure 5C). We observed a significant reduction in the frequency with which FANCD2 and γH2AX foci segregated asymmetrically following ATR or CHK1 inhibition in the mitotic phase, but not with ATM inhibition (Figures 5D, 5E, and S7B). We also confirmed that ATR/CHK1 inhibition in mitosis led to a reduction in the frequency of NDS (Figures 5F and S7D). Considering that ATR and CHK1 inhibitors are able to induce cell-cycle checkpoint override and cell death, which may affect the analysis of NDS, we performed additional experiments to examine mitotic progression after ATR/CHK1 inhibitor treatment. For this, we examined the percentage of cells in different M-phase stages at 10 min and 2 h after release from G2/M synchronization and found no significant difference (Figures S6A and S6B). Moreover, we did not detect any significant increase in the level of cell death after ATR/CHK1 inhibitor treatment for 2 h (Figure S6C). Taken together, these data suggest that replication-stress-induced asymmetric DDR protein segregation, which serves as a marker of NDS, is ATR-CHK1 dependent.

Nonrandom Chromatid Segregation Induces Genomic Instability and Cell Death in Damaged Daughter Cells

Because it is well established that DNA replication stress can activate cell-cycle arrest or cell death, we explored the fate of two different daughter cells that arise in cases of asymmetric distribution of the DDR (Palmieri et al., 2018). For

Please cite this article in press as: Xing et al., Replication Stress Induces ATR/CHK1-Dependent Nonrandom Segregation of Damaged Chromosomes, Molecular Cell (2020), https://doi.org/10.1016/j.molcel.2020.04.005

CellPress

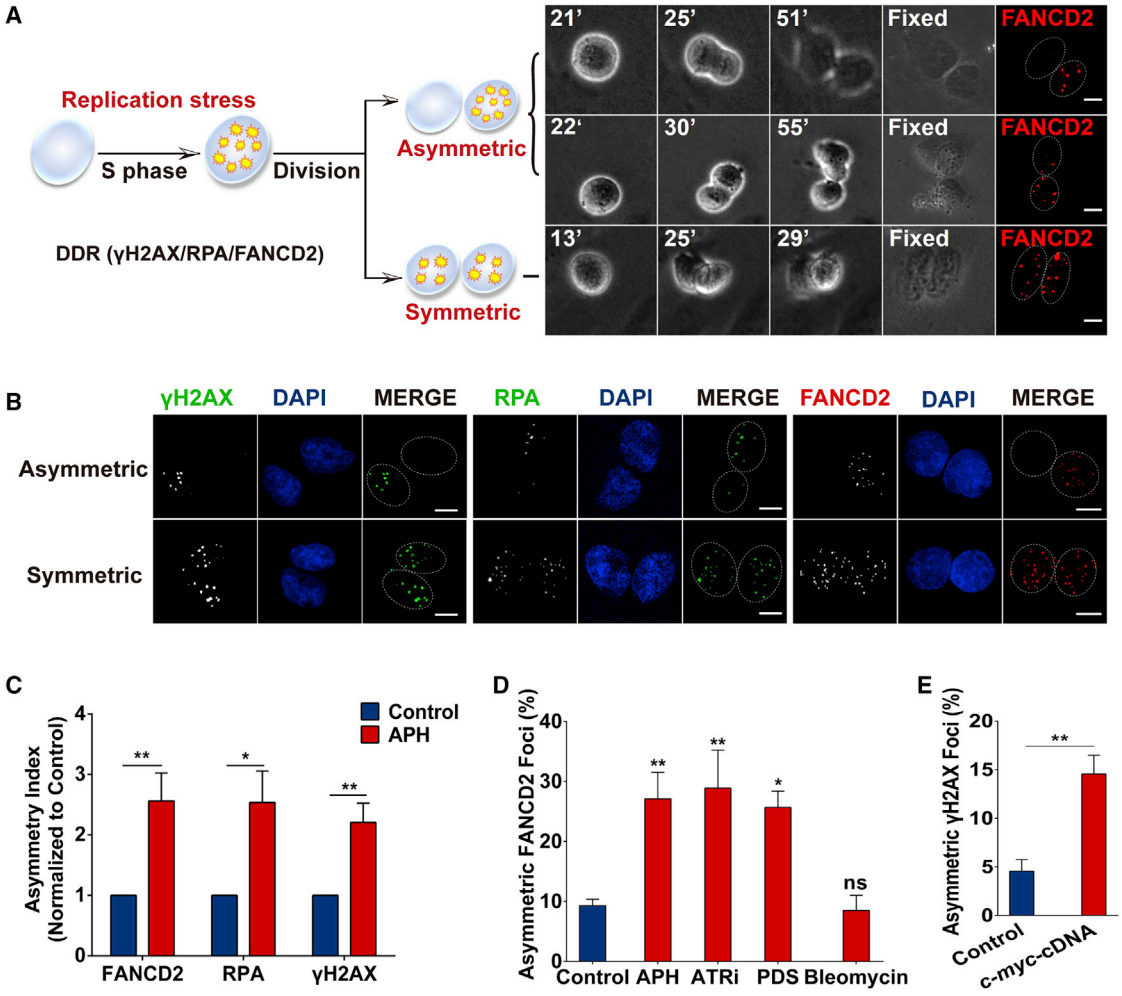

Figure 3. Replication Stress Induces Asymmetric Distribution of DDR Proteins

(A) Left: schematic representation of asymmetric and symmetric division of DDR proteins in daughter U2OS cells following replication stress. Right: still images of live-cell imaging showing the asymmetric and symmetric division of the DDR protein FANCD2. Asymmetric division of the DDR protein (e.g., FANCD2) is defined as the event that occurs in a pair of daughter cells (each containing more than 3 DDR protein foci) where the ratio of the number of foci in the two daughter cells is <0.4. Scale bars, 10 μm.

(B) Immunofluorescence images of the asymmetric and symmetric division of the DDR proteins γH2AX, RPA, and FANCD2. Scale bars, 10 μm.

(C) Bar graph showing an increased asymmetry index (the asymmetry index is defined as the ratio of the percentage of DDR protein asymmetry in the APH-induced group compared to that in the control group) of the DDR following APH-induced replication stress. More than 300 G1 daughter pairs were counted for each condition.

(D) The frequency of asymmetric division of FANCD2 foci in daughter cells with replication stress induced by different agents (APH, an ATR inhibitor [ATRi], and PDS). Bleomycin was included as a DNA-damaging agent that generates little or no replication stress. More than 300 G1 daughter pairs were counted for each condition.

(E) Quantitative data showing that c-Myc overexpression induces more γH2AX asymmetry of primary MEFs, and at least 500 G1 daughter pairs were counted in each condition.

Data are the mean ± SEM from three independent experiments. *$p < 0.05$; **$p < 0.01$; ns, not significant; two-way ANOVA (C), one-way ANOVA (D), or t test (E).

this, we generated a cell line with stable expression of both RPA-mCherry and histone H2B-GFP. Using both live cell imaging and an immunofluorescence assay, we demonstrated that NDS (through following CldU-labeled DNA) was accompanied by an accumulation of micronuclei (Figures 6A and S7F). A similar phenomenon was observed in those cells where RPA foci segregated asymmetrically (Figure 6B). Interestingly, inhibition of CHK1 in mitosis suppressed not only asymmetric DNA segregation but also micronucleus formation and other manifestations of APH-induced chromosome instability (chromatin bridges and lagging chromatin; Figure 6C). These data suggest that asymmetric segregation of DNA promotes genomic instability in at least one of the affected daughter cells. To address this issue more directly, we followed individual cells over two cell cycles by live imaging. We observed that those mother cells that underwent

Please cite this article in press as: Xing et al., Replication Stress Induces ATR/CHK1-Dependent Nonrandom Segregation of Damaged Chromosomes, Molecular Cell (2020), https://doi.org/10.1016/j.molcel.2020.04.005

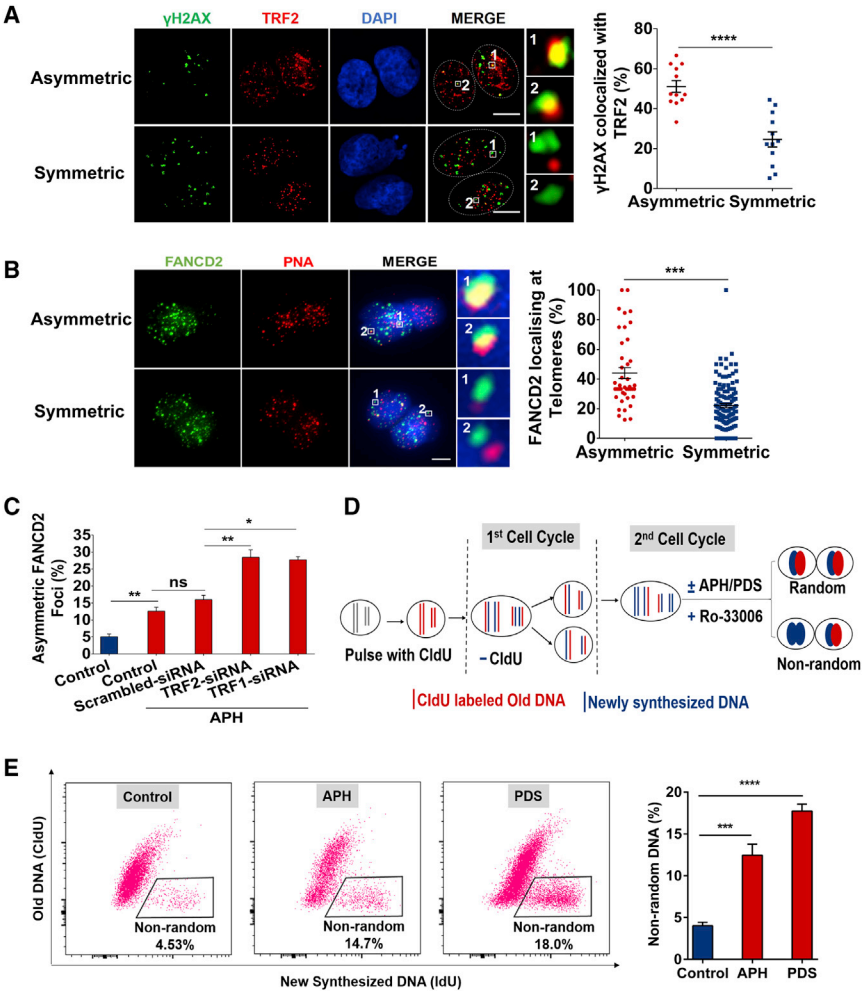

Figure 4. Telomeric Replication Stress Preferentially Induces Asymmetric DDR and NDS

(A) Representative images and quantification of asymmetrically or symmetrically segregated γH2AX foci that co-localize with TRF2. Scale bars, 10 μm. 12 G1 daughter pairs were counted for each condition.

(B) Representative images and quantification of asymmetrically (n = 42) or symmetrically (n = 123) segregated FANCD2 foci that co-localize with a telomeric PNA probe. Scale bars, 10 μm.

(C) Quantification of asymmetrically segregated FANCD2 foci in daughter cell pairs after small interfering RNA (siRNA)-mediated depletion of TRF2 or TRF1 and APH treatment in S phase. More than 300 G1 daughter pairs were counted for each condition.

(D) Schematic representation of (E). Cells were pulsed with CldU (red) for 2 weeks. During the second cell division following removal of CldU, IdU (blue) was added, and the IdU-labeled new DNA strands were then segregated either randomly (random) or exclusively to one of the daughter cells (nonrandom) under each condition.

(E) U2OS daughter cells in G1 (Cyclin A negative) were gated and sorted into CldU positive and IdU positive fractions, and then analyzed for the percentage of nonrandom segregation (only IdU-labeled DNA) by flow cytometry. Left: Representative FACS images of control and APH/PDS-treated cells. Right: Quantification of the data from left. At least 20000 cells were analyzed in each condition. Data are the mean ± SEM from three independent experiments. *$p < 0.05$, **$p < 0.01$, ***$p < 0.001$, ****$p < 0.0001$, ns, not significant, t test (A-B), one-way ANOVA (C and D).

asymmetric inheritance in the first cell division generated two daughter cells with different fates; the daughter cells lacking RPA foci remained competent for continued proliferation, while the others retaining the RPA foci underwent cell-cycle arrest or apoptosis (Figures 6D–6F). These data suggest that a selective advantage exists for a cell population able to effect asymmetric segregation of damaged DNA in that it ensures the survival of at least one daughter cell.

DISCUSSION

It is well established that telomeres are particularly susceptible to replication stress and are hotspots for conducting DNA synthesis in mitosis (MiDAS) following APH treatment in S phase (Dilley et al., 2016; Min et al., 2019; Özer et al., 2018; Verma et al., 2019). When cancer cells suffer replication stress, ATR/CHK1 signaling tends to be persistently activated, thus inducing asymmetric inheritance of the damaged/undamaged DNA strands. The net result of this DDR-driven segregation asymmetry is the production of one relatively healthy cell that can continue to proliferate and one cell that is "sacrificed" (Figure 6G). Central to this model is the concept that damage generated by replication stress should be located predominantly on the newly replicated DNA strands and that this serves to distinguish them from the older (clean) template strands (Figures 2A–2C). This begs the question as to why the recently synthesized DNA is damaged in some way during the process of DNA replication while the older DNA template from an earlier cell cycle is not. We propose that the chromatid containing the younger template DNA strand is different because it is not synthesized during S phase by conventional DNA replication in those cases where the cell is experiencing replication stress. Instead, the DNA is synthesized during MiDAS or a related DNA repair process that occurs in the late G2/M phases, when the cell attempts to rescue regions of underreplicated DNA. Further, we propose that, because this repair process is likely to occur via break-induced replication (BIR), a process that is highly error prone, at least in yeast (Elango et al., 2017, 2018). If this model has validity, there must be a mechanism to differentiate the older template strand from the new one. One possible mechanism involves epigenetic marks that differentially decorate the template DNA strand and the nascent strand (Lansdorp, 2007). Another potential mechanism is that the DNA template synthesized in

Please cite this article in press as: Xing et al., Replication Stress Induces ATR/CHK1-Dependent Nonrandom Segregation of Damaged Chromosomes, Molecular Cell (2020), https://doi.org/10.1016/j.molcel.2020.04.005

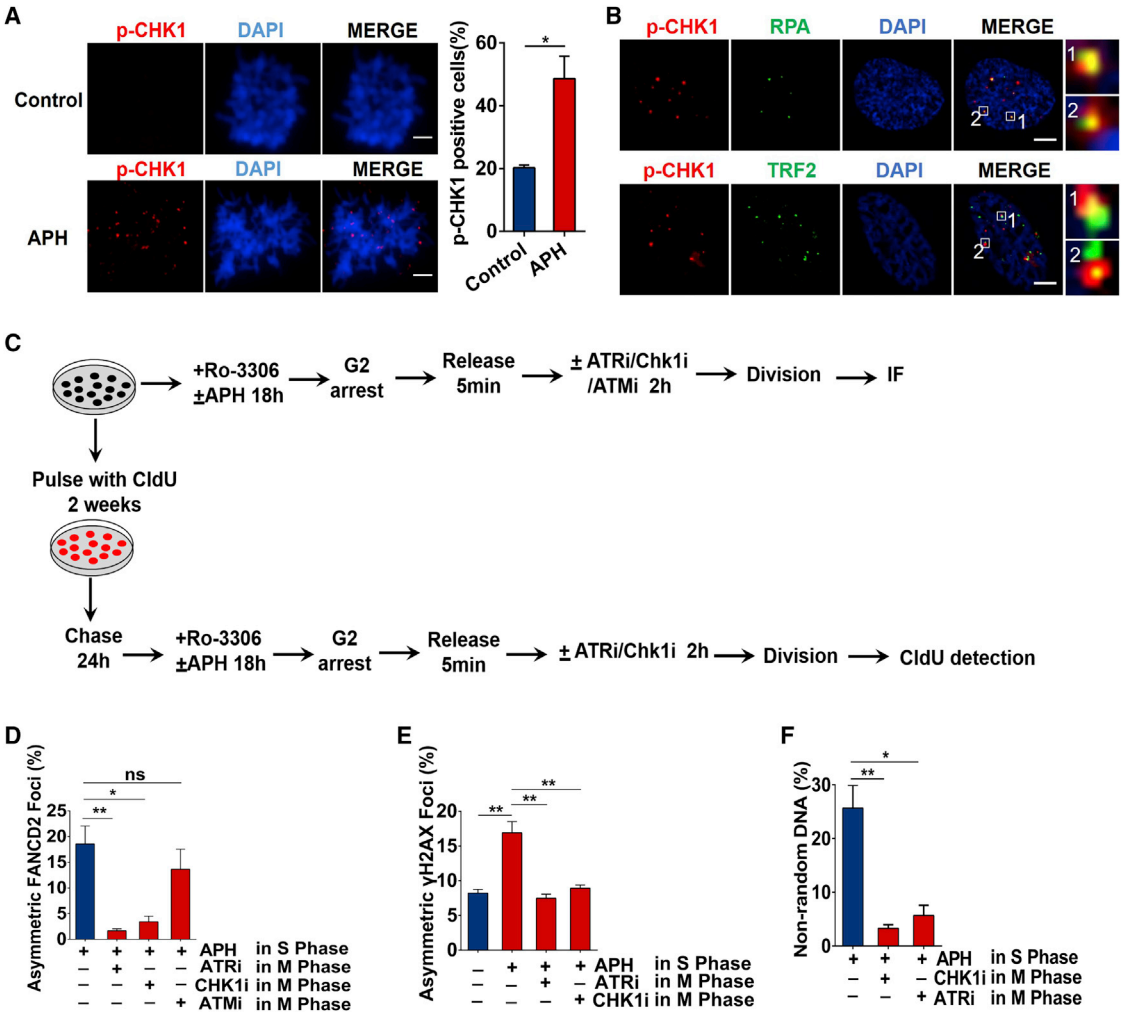

Figure 5. Replication Stress Induces ATR/CHK1-Dependent Asymmetric DDR and NDS

(A) Representative images and quantification of the phosphorylation of CHK1 in mitosis induced by APH. Scale bars, 5 μm. Cells with more than five phospho-CHK1 foci were counted as positive. More than 1,000 mitotic cells were counted in each condition.

(B) Representative images demonstrating that phospho-CHK1 co-localizes with RPA or TRF2 in mitosis. Scale bars, 5 μm.

(C) Experimental workflow for results described in (D)–(F). For CldU detection, cells were treated with APH in S phase and ATR, CHK, or ATM inhibitors in the second cell cycle after CldU labeling.

(D and E) Asymmetric FANCD2 foci (D) or asymmetric γH2AX foci (E) in daughter pairs from cells treated with APH in S phase and ATR, CHK, or ATM inhibitors in mitosis. More than 300 G1 daughter pairs were counted for each condition.

(F) The frequency of nonrandom distribution of DNA in cells chased two cell cycles after CldU labeling. At least 300 G1 daughter pairs were counted for each condition.

Data are the mean ± SEM from three independent experiments. *p < 0.05; **p < 0.01; ns, not significant; t test (A) or one-way ANOVA (D–F).

the previous cycle is more likely to contain replication-related errors, such as incorporation of incorrect bases, ribonucleotides, or oxidized bases, which may also serve as a marker to distinguish the newer template DNA strand from the older one. Interestingly, our data support the previous hypothesis of Gregory Charville and Thomas Rando that DNA damage caused by replication stress can generate signals for distinguishing old versus new sister chromatids during NDS (Charville and Rando, 2013).

In the context of tumorigenesis, our data support the notion that cancer cells might employ a set of tools to maintain genome stability, allowing the daughter cells to have as many "clean" old DNA strands as possible. However, this asymmetric segregation would inevitably also create daughter cells containing predominantly newly synthesized strands, which are more likely to have mutations or abnormal epigenetic modifications. Although most of the cells with "damaged" DNA would be expected not to survive, some might inadvertently acquire traits that provide a selective advantage, permitting the development of more aggressive or invasive tumors. Further work is warranted to analyze the fate of cells containing newly synthesized strands.

Please cite this article in press as: Xing et al., Replication Stress Induces ATR/CHK1-Dependent Nonrandom Segregation of Damaged Chromosomes, Molecular Cell (2020), https://doi.org/10.1016/j.molcel.2020.04.005

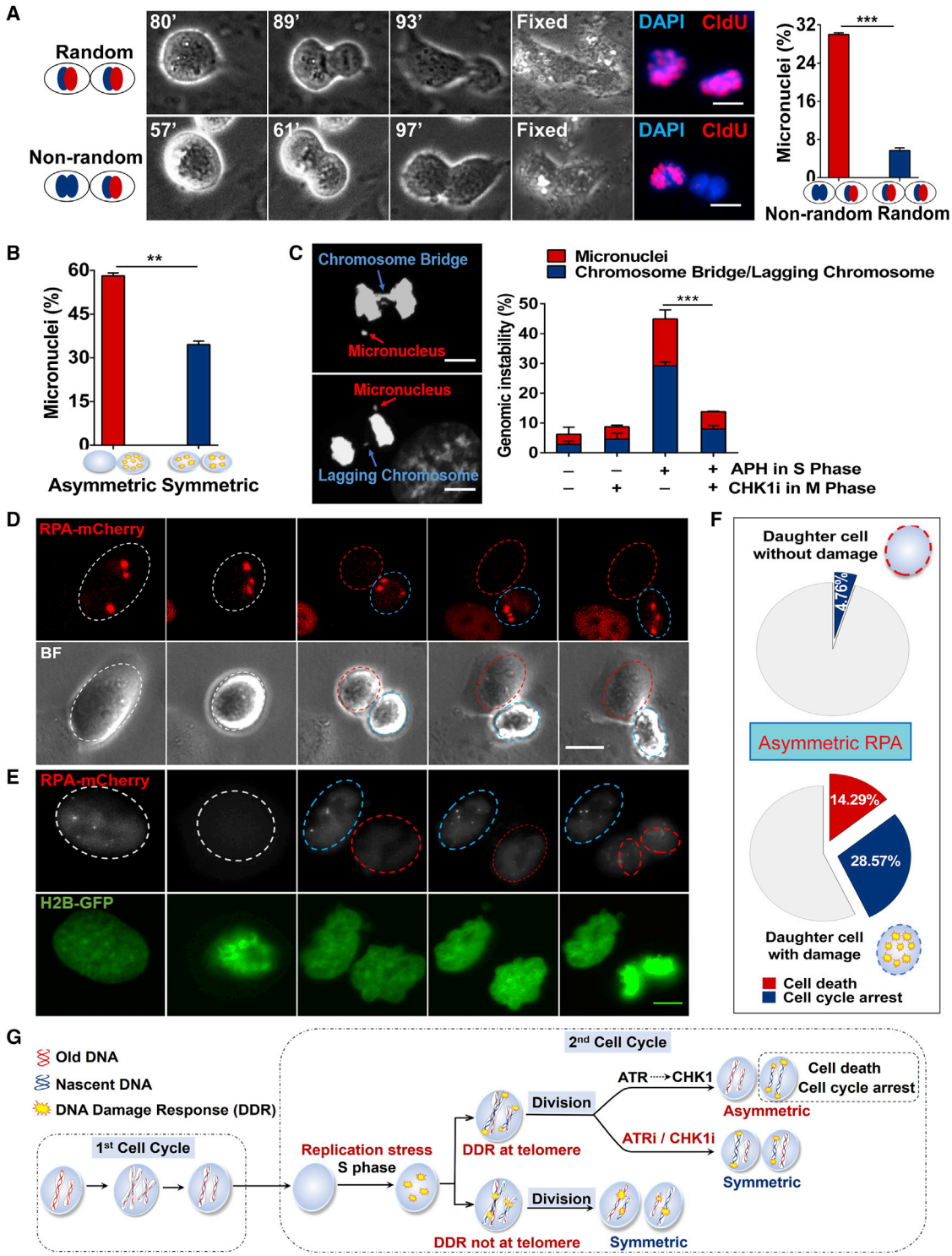

Figure 6. Nonrandom Chromatid Induces Genomic Instability and Cell Death in Damaged Daughter Cells

The cells were labeled and treated as described in Figure 1A.

(A) Left: representative still images from movies of dividing cells that contain a micronucleus and partition their CldU-labeled template DNA (red) either randomly to both daughter cells or exclusively to one of the daughter cells. Scale bars, 10 μm. Right: quantification of immunofluorescence data of G1 daughter pairs showing either nonrandom (n = 105) or random (n = 320) segregation of CldU-labeled DNA.

(B) Quantification of live-cell imaging data of dividing cells (n = 69) showing either asymmetric or symmetric segregation of RPA foci.

(legend continued on next page)

STAR★METHODS

Detailed methods are provided in the online version of this paper and include the following:

- KEY RESOURCES TABLE
- RESOURCE AVAILABILITY
  - Lead Contact
  - Materials Availability
  - Data and Code Availability
- EXPERIMENTAL MODEL AND SUBJECT DETAILS
- METHOD DETAILS
  - RNA interference
  - Establishment of RPA-mCherry or H2B-GFP overexpression stable cell lines and c-MYC lentiviral infections
  - Cell synchronization and induction of replication stress using low-dose APH
  - Immunofluorescence and fluorescence microscopy
  - CldU administration and chase
  - Immunostaining
  - Combined immunofluorescence staining and FISH
  - Flow cytometry
  - RT-PCR
  - Western blot analysis
  - Live imaging
  - Analysis of mitotic defects
- QUANTIFICATION AND STATISTICAL ANALYSIS

SUPPLEMENTAL INFORMATION

Supplemental Information can be found online at https://doi.org/10.1016/j.molcel.2020.04.005.

ACKNOWLEDGMENTS

We thank Dr. Jingde Zhu in the "Gathering Wisdom to Strive" initiative. We also thank Dr. Chao Zhang, Dr. Xinwei Geng, and Dr. Syeda Madiha Zahra for helpful comments on the manuscript. This research was funded by the Ministry of Science and Technology of the People's Republic of China (2016YFA0100301), the Natural Science Foundation of China (81870007, 81920108001), the Zhejiang Provincial Natural Science Foundation (LD19H160001), and the Zhejiang Provincial Program for the Cultivation of High-Level Innovative Health Talents (2016-63). I.D.H. is supported by the Danish National Research Foundation (DNRF115) and the Nordea Foundation.

AUTHOR CONTRIBUTIONS

S.Y. initiated, designed, and supervised the study. M.X., F.Z., H.L., S.C., L.C., H.Z., X.W., F.J., and G.C. performed the experiments and analyzed the data. M.X. wrote the article. S.Y., H.S., I.D.H., Y.L., Z.C., and W.L. helped design the experiments and edited the manuscript.

DECLARATION OF INTERESTS

The authors declare no competing interests.

Received: October 30, 2019
Revised: February 22, 2020
Accepted: April 6, 2020
Published: April 29, 2020

REFERENCES

Akera, T., Chmátal, L., Trimm, E., Yang, K., Aonbangkhen, C., Chenoweth, D.M., Janke, C., Schultz, R.M., and Lampson, M.A. (2017). Spindle asymmetry drives non-Mendelian chromosome segregation. Science *358*, 668–672.

Barker, N., van Es, J.H., Kuipers, J., Kujala, P., van den Born, M., Cozijnsen, M., Haegebarth, A., Korving, J., Begthel, H., Peters, P.J., and Clevers, H. (2007). Identification of stem cells in small intestine and colon by marker gene Lgr5. Nature *449*, 1003–1007.

Bartek, J., Bartkova, J., and Lukas, J. (2007). DNA damage signalling guards against activated oncogenes and tumour progression. Oncogene *26*, 7773–7779.

Bi, X., Srikanta, D., Fanti, L., Pimpinelli, S., Badugu, R., Kellum, R., and Rong, Y.S. (2005). Drosophila ATM and ATR checkpoint kinases control partially redundant pathways for telomere maintenance. Proc. Natl. Acad. Sci. USA *102*, 15167–15172.

Burke, D.J. (2013). Unbiased segregation of yeast chromatids in *Saccharomyces cerevisiae*. Chromosome Res. *21*, 193–202.

Cairns, J. (1975). Mutation selection and the natural history of cancer. Nature *255*, 197–200.

Chan, K.L., Palmai-Pallag, T., Ying, S., and Hickson, I.D. (2009). Replication stress induces sister-chromatid bridging at fragile site loci in mitosis. Nat. Cell Biol. *11*, 753–760.

Chang, J.T., Ciocca, M.L., Kinjyo, I., Palanivel, V.R., McClurkin, C.E., Dejong, C.S., Mooney, E.C., Kim, J.S., Steinel, N.C., Oliaro, J., et al. (2011). Asymmetric proteasome segregation as a mechanism for unequal partitioning of the transcription factor T-bet during T lymphocyte division. Immunity *34*, 492–504.

Charville, G.W., and Rando, T.A. (2011). Stem cell ageing and non-random chromosome segregation. Philos. Trans. R. Soc. Lond. B Biol. Sci. *366*, 85–93.

(C) Representative images (left) and quantification (right) of DAPI-positive bulky chromatin bridges, micronuclei, and lagging chromosomes in U2OS cells. APH was added in S phase, and the CHK1 inhibitor (CHK1i) was added in mitosis. Scale bars, 10 μm. At least 200 anaphase or G1 daughter pairs were counted for each condition.
(D) Representative still images from a live-cell imaging experiment showing the different fate of daughter cells that are DNA-damage positive (RPA-foci positive, cyan dotted line) or "undamaged" (RPA-foci negative, red dotted line). A dead, damaged daughter cell (RPA-foci positive, cyan dotted line) is shown. Scale bars, 10 μm.
(E) Cell-cycle arrest in a damaged daughter cell (marked by cyan dotted line). Scale bars, 10 μm.
(F) Quantification of the different fate of daughter cells from live-cell imaging data by tracking the extent of RPA focus asymmetry (n = 30).
(G) A cartoon showing how nonrandom sister chromatid segregation induces asymmetric segregation of DDR proteins (γH2AX, RPA, FANCD2). Cells were treated with CldU for 2 weeks to ensure that all parental DNA was labeled, and then the CldU was removed and the cells were allowed to progress through one cell cycle in CldU-free medium. During the second cell cycle, cells were treated with APH in S phase to induce replication stress. When the replication-stress-induced DDR occurs at a telomere, cells activate the ATR/CHK1 signaling pathway that leads to asymmetric segregation of DDR proteins to produce one healthy daughter and one damaged daughter (which either dies or shows cell-cycle arrest). In the presence of the ATR inhibitor or CHK1 inhibitor added in mitosis, DDR proteins segregate symmetrically. When the replication-stress-induced DDR proteins are localized to chromosome arms (non-telomeric loci), they are prone to symmetric division.
Data are the mean ± SEM from three independent experiments. $^{**}p < 0.01$, $^{***}p < 0.001$, t test (A and B) or one-way ANOVA (C).

Charville, G.W., and Rando, T.A. (2013). The mortal strand hypothesis: non-random chromosome inheritance and the biased segregation of damaged DNA. Semin. Cell Dev. Biol. *24*, 653–660.

Conboy, M.J., Karasov, A.O., and Rando, T.A. (2007). High incidence of non-random template strand segregation and asymmetric fate determination in dividing stem cells and their progeny. PLoS Biol. *5*, e102.

Denoth-Lippuner, A., Krzyzanowski, M.K., Stober, C., and Barral, Y. (2014). Role of SAGA in the asymmetric segregation of DNA circles during yeast ageing. eLife *3*, e.03790.

Derivery, E., Seum, C., Daeden, A., Loubéry, S., Holtzer, L., Jülicher, F., and Gonzalez-Gaitan, M. (2015). Polarized endosome dynamics by spindle asymmetry during asymmetric cell division. Nature *528*, 280–285.

Dilley, R.L., Verma, P., Cho, N.W., Winters, H.D., Wondisford, A.R., and Greenberg, R.A. (2016). Break-induced telomere synthesis underlies alternative telomere maintenance. Nature *539*, 54–58.

Elango, R., Sheng, Z., Jackson, J., DeCata, J., Ibrahim, Y., Pham, N.T., Liang, D.H., Sakofsky, C.J., Vindigni, A., Lobachev, K.S., et al. (2017). Break-induced replication promotes formation of lethal joint molecules dissolved by Srs2. Nat. Commun. *8*, 1790.

Elango, R., Kockler, Z., Liu, L., and Malkova, A. (2018). Investigation of break-induced replication in yeast. Methods Enzymol. *601*, 161–203.

Escobar, M., Nicolas, P., Sangar, F., Laurent-Chabalier, S., Clair, P., Joubert, D., Jay, P., and Legraverend, C. (2011). Intestinal epithelial stem cells do not protect their genome by asymmetric chromosome segregation. Nat. Commun. *2*, 258.

Freida, D., Lecourt, S., Cras, A., Vanneaux, V., Letort, G., Gidrol, X., Guyon, L., Larghero, J., and Thery, M. (2013). Human bone marrow mesenchymal stem cells regulate biased DNA segregation in response to cell adhesion asymmetry. Cell Rep. *5*, 601–610.

Gallo, C.M., Wang, J.T., Motegi, F., and Seydoux, G. (2010). Cytoplasmic partitioning of P granule components is not required to specify the germline in C. elegans. Science *330*, 1685–1689.

Ginda, K., Santi, I., Bousbaine, D., Zakrzewska-Czerwińska, J., Jakimowicz, D., and McKinney, J. (2017). The studies of ParA and ParB dynamics reveal asymmetry of chromosome segregation in mycobacteria. Mol. Microbiol. *105*, 453–468.

Gravel, A., Dubuc, I., Wallaschek, N., Gilbert-Girard, S., Collin, V., Hall-Sedlak, R., Jerome, K.R., Mori, Y., Carbonneau, J., Boivin, G., et al. (2017). Cell culture systems to study human herpesvirus 6A/B chromosomal integration. J. Virol. *91*, e00437-17.

Habib, S.J., Chen, B.C., Tsai, F.C., Anastassiadis, K., Meyer, T., Betzig, E., and Nusse, R. (2013). A localized Wnt signal orients asymmetric stem cell division in vitro. Science *339*, 1445–1448.

Karpowicz, P., Morshead, C., Kam, A., Jervis, E., Ramunas, J., Cheng, V., and van der Kooy, D. (2005). Support for the immortal strand hypothesis: neural stem cells partition DNA asymmetrically in vitro. J. Cell Biol. *170*, 721–732.

Katajisto, P., Döhla, J., Chaffer, C.L., Pentinmikko, N., Marjanovic, N., Iqbal, S., Zoncu, R., Chen, W., Weinberg, R.A., and Sabatini, D.M. (2015). Stem cells. Asymmetric apportioning of aged mitochondria between daughter cells is required for stemness. Science *348*, 340–343.

Kiel, M.J., He, S., Ashkenazi, R., Gentry, S.N., Teta, M., Kushner, J.A., Jackson, T.L., and Morrison, S.J. (2007). Haematopoietic stem cells do not asymmetrically segregate chromosomes or retain BrdU. Nature *449*, 238–242.

Knoblich, J.A. (2010). Asymmetric cell division: recent developments and their implications for tumour biology. Nat. Rev. Mol. Cell Biol. *11*, 849–860.

Kressmann, S., Campos, C., Castanon, I., Fürthauer, M., and González-Gaitán, M. (2015). Directional Notch trafficking in Sara endosomes during asymmetric cell division in the spinal cord. Nat. Cell Biol. *17*, 333–339.

Lansdorp, P.M. (2007). Immortal strands? Give me a break. Cell *129*, 1244–1247.

Liu, W., Jeganathan, G., Amiri, S., Morgan, K.M., Ryan, B.M., and Pine, S.R. (2013). Asymmetric segregation of template DNA strands in basal-like human breast cancer cell lines. Mol. Cancer *12*, 139.

Lopez-Vernaza, M.A., and Leach, D.R. (2013). Symmetries and asymmetries associated with non-random segregation of sister DNA strands in Escherichia coli. Semin. Cell Dev. Biol. *24*, 610–617.

Magdalou, I., Lopez, B.S., Pasero, P., and Lambert, S.A. (2014). The causes of replication stress and their consequences on genome stability and cell fate. Semin. Cell Dev. Biol. *30*, 154–164.

Min, J., Wright, W.E., and Shay, J.W. (2017). Alternative lengthening of telomeres mediated by mitotic DNA synthesis engages break-induced replication processes. Mol. Cell. Biol. *37*, e00226-17.

Min, J., Wright, W.E., and Shay, J.W. (2019). Clustered telomeres in phase-separated nuclear condensates engage mitotic DNA synthesis through BLM and RAD52. Genes Dev. *33*, 814–827.

Morales, C.P., Holt, S.E., Ouellette, M., Kaur, K.J., Yan, Y., Wilson, K.S., White, M.A., Wright, W.E., and Shay, J.W. (1999). Absence of cancer-associated changes in human fibroblasts immortalized with telomerase. Nat. Genet. *21*, 115–118.

Özer, Ö., Bhowmick, R., Liu, Y., and Hickson, I.D. (2018). Human cancer cells utilize mitotic DNA synthesis to resist replication stress at telomeres regardless of their telomere maintenance mechanism. Oncotarget *9*, 15836–15846.

Palmieri, D., Tessari, A., and Coppola, V. (2018). Scorpins in the DNA damage response. Int. J. Mol. Sci. *19*, E1794.

Pine, S.R., Ryan, B.M., Varticovski, L., Robles, A.I., and Harris, C.C. (2010). Microenvironmental modulation of asymmetric cell division in human lung cancer cells. Proc. Natl. Acad. Sci. USA *107*, 2195–2200.

Potten, C.S., Hume, W.J., Reid, P., and Cairns, J. (1978). The segregation of DNA in epithelial stem cells. Cell *15*, 899–906.

Rando, T.A. (2007). The immortal strand hypothesis: segregation and reconstruction. Cell *129*, 1239–1243.

Rebollo, E., Sampaio, P., Januschke, J., Llamazares, S., Varmark, H., and González, C. (2007). Functionally unequal centrosomes drive spindle orientation in asymmetrically dividing Drosophila neural stem cells. Dev. Cell *12*, 467–474.

Rocheteau, P., Gayraud-Morel, B., Siegl-Cachedenier, I., Blasco, M.A., and Tajbakhsh, S. (2012). A subpopulation of adult skeletal muscle stem cells retains all template DNA strands after cell division. Cell *148*, 112–125.

Schnabl, B., Choi, Y.H., Olsen, J.C., Hagedorn, C.H., and Brenner, D.A. (2002). Immortal activated human hepatic stellate cells generated by ectopic telomerase expression. Lab. Invest. *82*, 323–333.

Shinin, V., Gayraud-Morel, B., Gomès, D., and Tajbakhsh, S. (2006). Asymmetric division and cosegregation of template DNA strands in adult muscle satellite cells. Nat. Cell Biol. *8*, 677–687.

Sotiropoulou, P.A., Candi, A., and Blanpain, C. (2008). The majority of multipotent epidermal stem cells do not protect their genome by asymmetrical chromosome segregation. Stem Cells *26*, 2964–2973.

Stagno D'Alcontres, M., Mendez-Bermudez, A., Foxon, J.L., Royle, N.J., and Salomoni, P. (2007). Lack of TRF2 in ALT cells causes PML-dependent p53 activation and loss of telomeric DNA. J. Cell Biol. *179*, 855–867.

Thaunat, O., Granja, A.G., Barral, P., Filby, A., Montaner, B., Collinson, L., Martinez-Martin, N., Harwood, N.E., Bruckbauer, A., and Batista, F.D. (2012). Asymmetric segregation of polarized antigen on B cell division shapes presentation capacity. Science *335*, 475–479.

Tran, V., Lim, C., Xie, J., and Chen, X. (2012). Asymmetric division of Drosophila male germline stem cell shows asymmetric histone distribution. Science *338*, 679–682.

Verbist, K.C., Guy, C.S., Milasta, S., Liedmann, S., Kamiński, M.M., Wang, R., and Green, D.R. (2016). Metabolic maintenance of cell asymmetry following division in activated T lymphocytes. Nature *532*, 389–393.

Verma, P., Dilley, R.L., Zhang, T., Gyparaki, M.T., Li, Y., and Greenberg, R.A. (2019). RAD52 and SLX4 act nonepistatically to ensure telomere stability during alternative telomere lengthening. Genes Dev. *33*, 221–235.

Yadlapalli, S., and Yamashita, Y.M. (2013). Chromosome-specific nonrandom sister chromatid segregation during stem-cell division. Nature *498*, 251–254.

Yang, J., McCormick, M.A., Zheng, J., Xie, Z., Tsuchiya, M., Tsuchiyama, S., El-Samad, H., Ouyang, Q., Kaeberlein, M., Kennedy, B.K., and Li, H. (2015). Systematic analysis of asymmetric partitioning of yeast proteome between mother and daughter cells reveals "aging factors" and mechanism of lifespan asymmetry. Proc. Natl. Acad. Sci. USA *112*, 11977–11982.

Zhang, D., Wang, Y., and Zhang, S. (2014). Asymmetric cell division in polyploid giant cancer cells and low eukaryotic cells. BioMed Res. Int. *2014*, 432652.

Zimdahl, B., Ito, T., Blevins, A., Bajaj, J., Konuma, T., Weeks, J., Koechlein, C.S., Kwon, H.Y., Arami, O., Rizzieri, D., et al. (2014). Lis1 regulates asymmetric division in hematopoietic stem cells and in leukemia. Nat. Genet. *46*, 245–252.

Please cite this article in press as: Xing et al., Replication Stress Induces ATR/CHK1-Dependent Nonrandom Segregation of Damaged Chromosomes, Molecular Cell (2020), https://doi.org/10.1016/j.molcel.2020.04.005

STAR★METHODS

KEY RESOURCES TABLE

REAGENT or RESOURCE	SOURCE	IDENTIFIER
Antibodies		
Rabbit anti-FANCD2	Abcam	Cat#ab108928; RRID: AB_10862535
Rabbit anti-FANCD2	Novus	Cat#NB100-182; RRID: AB_1108498
Mouse anti-Ser139-phosphorylated H2A.X	Millipore	Cat#05-636; RRID: AB_309864
Rabbit anti-phospho-RPA	Abcam	Cat#ab109394; RRID: AB_10860648
Rabbit anti-phospho-CHK1	Abcam	Cat#ab47318; RRID: AB_869137
Mouse anti-cyclin A	Santa Cruz	Cat#sc-752; RRID: AB_2072134
Mouse anti-TRF2	Abcam	Cat#ab13579; RRID: AB_300474
Rabbit anti-TRF2	Abcam	Cat#ab108997; RRID: AB_10866674
Rabbit anti-TRF1	Abcam	Cat#ab236061
Mouse anti-TRF1	Abcam	Cat#ab10579; RRID: AB_2201461
Mouse anti-PML	Abcam	Cat#ab96051; RRID: AB_10679887
Anti-UBF	Abcam	Cat#ab244287
APC-BrdU antibody	BioLegend	Cat#339807; RRID: AB_10900446
Anti-BrdU antibody BU1/75	Abcam	Cat#ab6326; RRID: AB_305426
Mouse anti-BrdU antibody B44	BD Biosciences	Cat#347580; RRID: AB_400326
Anti-rabbit IgG, HRP-linked Antibody	Cell Signaling Technology	Cat#7074; RRID: AB_2099233
Anti-mouse IgG, HRP-linked Antibody	Cell Signaling Technology	Cat#7076; RRID: AB_330924
β-Actin-HRP Rabbit Monoclonal Antibody	Beyotime	Cat#AF5006
Alexa Fluor 488 goat anti-Rabbit	Life Technologies	Cat#A-11034; RRID: AB_2576217
Alexa Fluor 568 goat anti-Rabbit	Life Technologies	Cat#A-11036; RRID: AB_143011
Alexa Fluor 568 goat anti-Mouse	Life Technologies	Cat#A-11031; RRID: AB_144696
Alexa Fluor 488 goat anti-Mouse	Life Technologies	Cat#A-11029; RRID: AB_138404
Alexa Fluor 594 goat anti-Rat	Abcam	Cat#Ab150160; RRID: AB_2756445
Chemicals, Peptides, and Recombinant Proteins		
RO3306	Selleck	Cat#S7747
Aphidicolin	Sigma	Cat#38966-21-1
ATR inhibitor	Selleck	Cat#S7050
CHK1 inhibitor	Selleck	Cat#S1532
ATM Kinase inhibitor	Selleck	Cat#S1092
Pyridostatin (PDS)	Selleck	Cat#S7444
Bleomycin	Selleck	Cat#S1214
Etoposide	Selleck	Cat#S1225
3,3′-Diaminobenzidine (DAB)	Beyotime	Cat#P0203
Triton X-100	Sangon Biotech	Cat#9002-93-1
BSA, Bovine Serum Albumin	Sangon Biotech	Cat#9048-46-8
PMSF, Phenylmethylsulfonyl fluoride	Roche	Cat#329-98-6
SDS	Sigma	Cat#151-21-3
Trizol	Invitrogen	Cat#15596018
Lipofectamine 2000 Transfection Reagent	Life Technologies	Cat#11668019
Neomycin	Selleck	Cat#S2568
Opti-MEM	GIBCO	Cat#31985-062
Polyethylenimine	Polysciences	Cat#23966-2

(*Continued on next page*)

Please cite this article in press as: Xing et al., Replication Stress Induces ATR/CHK1-Dependent Nonrandom Segregation of Damaged Chromosomes, Molecular Cell (2020), https://doi.org/10.1016/j.molcel.2020.04.005

Continued

REAGENT or RESOURCE	SOURCE	IDENTIFIER
Critical Commercial Assays		
MycoAlert™ Mycoplasma Detection Kit	Lonza	Cat#LT07-318
PNA telomere probe	PANAGENE	Cat#F1002
Deposited Data		
Original data	This paper	https://doi.org/10.17632/z9kt7w4myd.1
Experimental Models: Cell Lines		
U-2 OS	ATCC	ATCC ® HTB-96
293T	Chinese Academy of Sciences Cell Bank	SCSP-502
HeLa	Chinese Academy of Sciences Cell Bank	TCHu187
HCT116	ATCC	ATCC® CCL-247
MEF	ATCC	ATCC ® SCRC-1040
HFF-1	Chinese Academy of Sciences Cell Bank	SCSP-656
A549	Chinese Academy of Sciences Cell Bank	TCHu150
Oligonucleotides		
siCtrl: 5′-UCUCCGAACGUGUCACGUTT-3′	GenePharma	N/A
siTRF2: 5′-GAGGAUGAACUGUUUCAAGTT-3′	GenePharma	Stagno D'Alcontres et al., 2007
siTRF1: 5′-CGCAGAGGCUAUUAUUCAUTT-3′	GenePharma	N/A
Actin-forward: 5′-TGCTAGGAGCCAGAGCAGTA-3′	TSINGKE Biological Technology	N/A
Actin-reverse: 5′-AGTGTGACGTTGACATCCGT-3′	TSINGKE Biological Technology	N/A
TRF1-forward: 5′-TGCCGACCCTACTGAGGAG-3′	TSINGKE Biological Technology	N/A
TRF1- reverse: 5′-GCAGAGGAAATCGAGCATCCA-3′	TSINGKE Biological Technology	N/A
TRF2-forward: 5′-GTACGGGGACTTCAGACAGAT-3′	TSINGKE Biological Technology	N/A
TRF2-reverse: 5′-CGCGACAGACACTGCATAAC-3′	TSINGKE Biological Technology	N/A
Recombinant DNA		
pENTER cloning vectors	Life Technologies	11813-011
pc-myc	HANBIO	pHBLV000144
RPA-mcherry	This paper	N/A
psPAX2	This paper	N/A
pMD2.G	This paper	N/A
Software and Algorithms		
ImageJ (used for analysis of immunofluorescence microscopy images)	ImageJ Software	N/A
GraphPad Prism 6	GraphPad Software	N/A
NIS-Elements (used for capturing or exporting immunofluorescence microscopy images)	Nikon Elements software	N/A
ZEN (used for capturing or exporting immunofluorescence microscopy images)	ZEN software	N/A
OLYPUS FV31S-SW (used for capturing or exporting immunofluorescence microscopy images)	OLYPUS FV31S-SW software	N/A

RESOURCE AVAILABILITY

Lead Contact

Further information and requests for resources and reagents should be directed to and will be fulfilled by the Lead Contact, Songmin Ying (yings@zju.edu.cn).

Materials Availability

Source of cell lines used in the study is reported in the Key Resources Table. All unique/stable reagents generated in this study are available with an MTA.

Please cite this article in press as: Xing et al., Replication Stress Induces ATR/CHK1-Dependent Nonrandom Segregation of Damaged Chromosomes, Molecular Cell (2020), https://doi.org/10.1016/j.molcel.2020.04.005

Data and Code Availability

Original imaging data (microscopy as well as gels and blots) have been deposited to Mendeley Data and are available at https://doi.org/10.17632/z9kt7w4myd.1.

EXPERIMENTAL MODEL AND SUBJECT DETAILS

Cell lines including U-2OS, A549, HeLa and 293T were cultured in Dulbecco's modified Eagle's medium (DMEM; Hyclone) supplemented with 10% fetal bovine serum (FBS; Excell). Primary MEF and HFF-1 were grown in DMEM supplemented with 10% FBS, Glutamax (GIBCO, 35050-061) and non-essential amino acids (GIBCO, 11140-050). The cell lines HCT116 and MEF were grown in DMEM supplemented with 10% FBS. All cells were cultured at 37°C under a humidified atmosphere containing 5% carbon dioxide and subjected to monthly mycoplasma testing (using MycoAlert; Lonza) and found to be negative.

METHOD DETAILS

RNA interference

For knockdown experiments, cells were transfected 24–72 h before sample collection with the indicated siRNA using GenMute siRNA Transfection Reagent (SL100568, SignaGen Laboratories) according to the manufacturer's instructions:

Scrambled siRNA: (5′-UUCUCCGAACGUGUCACGUTT-3′),
TRF2 siRNA: (5′-GAGGAUGAACUGUUUCAAGTT-3′),
TRF1 siRNA: (5′-CGCAGAGGCUAUUAUUCAUTT-3′).

Establishment of RPA-mCherry or H2B-GFP overexpression stable cell lines and c-MYC lentiviral infections

RPA-mCherry cDNA was cloned into pENTER cloning vectors (Life Technologies). Final constructs were verified by sequencing. The *RPA-mCherry* construct was transfected into U-2OS cells using lipofectamine 2000 (Life Technologies). Stable cell lines were established by FACS sorting to isolate cells with high expression levels of m-Cherry and then maintained after neomycin (G418) antibiotic selection. Stable cell line with RPA-mCherry and H2B-GFP co-overexpression was conducted in the same way, and neomycin (G418) was also used to select cells with H2B-GFP cDNA expression.

The *c-myc-GFP* cDNA and lentivirus package vector plasmids psPAX2 and pMD2.G were purchased from HANBIO (Shanghai, China). Lentiviruses were produced in 293T cells using standard methods. Briefly, 293T cells were plated at 70%–80% confluency and were transfected using modified polyethylenimine (PEI) transfection method as follows. The medium of a 10-cm dish was replaced with 9 mL fresh DMEM medium. A mixture of 15 μg plasmid and 960 μL Opti-MEM (GIBCO) was mixed vigorously after adding 45 μL PEI (Polysciences, 1 mg/ml) and was incubated at room temperature for 10 min, and then was added into the medium in the 10-cm dish. The supernatant of the transfected 293T cells were harvested using a syringe and filtered through a 0.22 μm filter. Cells were infected with lentivirus containing media in the presence of polybrene.

Cell synchronization and induction of replication stress using low-dose APH

For synchronization in S phase, cells were cultured in the presence of 2 mM thymidine for 18 hours, followed by 3x washing with PBS. Cells were synchronized in late G2 phase of the cell cycle by incubation with 9 μM RO3306 for 16 h. Where stated, 0.3 μM APH (termed low-dose APH) was added for 16 h. Cells synchronized in G2 were subsequently washed with 1 × PBS for 5 min and allowed to progress for a further 30 min into prometaphase before mitotic shake off. For collection of anaphase cells or early G1 daughter cells, pelleted prometaphase cells were re-seeded onto either poly-lysine-coated glass coverslips (WHB) and incubated at 37°C in an atmosphere of 5% CO2 and allowed to progress into anaphase for a further 20 min or into the subsequent G1 phase for a further 140 min.

Immunofluorescence and fluorescence microscopy

For quantification of nuclear foci, cells were seeded in 12-well plates and treated as indicated before fixation in 4% formaldehyde containing 0.1% Triton X-100 (Sigma) at room temperature (RT) for 15 minutes. Fixed samples were permeabilized and blocked for at least 1 hour (with 0.5% Triton X-100 and 3% BSA in PBS) or stored at 4°C until use. The samples were incubated with indicated primary antibodies at 4°C overnight. The incubations with secondary antibodies conjugated to Alexa Fluor 488 or 555 (Life Technologies) was performed at RT for 1 hour followed by staining for DAPI. Images were visualized using either an automated Nikon Eclipse Ti microscope with Nikon Elements software (Nikon Instruments) or a high-resolution laser Confocal Microscope. DAPI was used to visualize the nuclei.

CldU administration and chase

CldU was added to the culture medium at a concentration of 1 μM for 2 weeks to label U-2OS, A549, HCT116, HeLa and MEF cell lines (Pine et al., 2010). For primary HFF-1 cells, which can only be cultured *in vitro* for a limited time, CldU was added to the culture

Please cite this article in press as: Xing et al., Replication Stress Induces ATR/CHK1-Dependent Nonrandom Segregation of Damaged Chromosomes, Molecular Cell (2020), https://doi.org/10.1016/j.molcel.2020.04.005

medium at a concentration of 1 μM for for 72h (Karpowicz et al., 2005). During the pulse, the medium was supplemented with fresh CldU every 72 h, and cell growth was maintained in log phase. For the single mitotic cell assays, cells were cultured for two weeks and then cultured in the absence of CldU (the chase) for two cell cycles followed by mitotic shake-off. Unless specified otherwise, mitotic shake-offs were performed when the cells were at 60%–90% confluence.

Immunostaining

To reveal CldU-labeled DNA, cells were fixed in cold 70% ethanol and incubated in 2 N HCl containing 0.5% Triton X-100 for 1 hour. After two washes in 0.5% Triton X-100/0.5% BSA and one wash in 0.5% Triton X-100/0.1% BSA, cells were blocked in PBS containing 0.5% Triton X-100/5% BSA for 1 hour, then incubated with a 1:1000 dilution of rat monoclonal antibody BU1/75 (ab6326, Abcam) for more than 12 hours at 4°C. Cells were then washed and incubated with a 1:2000 dilution of anti-rat Alexa Fluor 594 (ab150160, Abcam) for 1 hour at room temperature. After washing cells were mounted with DAPI to label the nuclei.

For the time-lapse imaging experiments, CldU-pulsed cells were plated onto poly-L-lysine–coated glass slides and cultured for two cell divisions. Then stained with CldU as above.

Combined immunofluorescence staining and FISH

Cells were cultured for about 2-3h when most cell were in Telophase after mitotic shake-off. Then cells were fixed and subjected to immunofluorescence staining as described above. After washing, samples were re-fixed in paraformaldehyde (4%) at 4°C for 10 min. Following ethanol dehydration, samples were denatured along with the PNA telomere probe (PANAGENE) at 85°C for 5 min. Slides were then incubated in a humidified chamber at 37°C for 2 h. DNA was counterstained with DAPI.

Flow cytometry

For flow cytometric analysis of the phosphorylation level of CHK1, cells were cultured with or without APH, and synchronized to G2/M phase with RO-3306 for 16h. With three washes, cells were harvested after release for 1h and fixed for 15 min with 4% formaldehyde/PBS. Cells were washed with 3% BSA/PBS, pH 7.4, permeabilized with 3% BSA/PBS and stained with phospho-CHK1 and then DAPI. Samples were analyzed on a cytoflex (Beckman Coulter).

For flow cytometric analysis of CldU and IdU, cells were labeled with CldU for 2 weeks, and then removed CldU and chased for 2 cell cycles with IdU. During the chase process, cells were exposed to APH and RO-3306 as the protocol described. Then cells were harvested after release to G1 phase and stained with Cyclin A, CldU (anti-BrdU rat monoclonal antibody BU1/75, which is known to stain for CldU but not for IdU), and IdU (mouse monoclonal antibody B44, which is known to stain for IdU but not for CldU under optimal staining conditions) (Pine et al., 2010). The Cyclin A negative, CldU negative and IdU positive cells were defined as the new-synthesized DNA resulting from non-random chromatid segregation.

RT-PCR

Cells were collected after transfection with siRNA for 24-72h, and immediately lysed using Trizol (Invitrogen). RNA extraction was isolated by phenol–chloroform extraction and then reversed for cDNAs. Transcripts of interest were quantified with real-time qPCR amplification. All the experiments were repeated for three times. The primers used in the qRT-PCR assays were as follows.

Actin-F: 5′-TGCTAGGAGCCAGAGCAGTA-3′
Actin-R: 5′-AGTGTGACGTTGACATCCGT-3′
TRF1-F: 5′-TGCCGACCCTACTGAGGAG-3′
TRF1-R: 5′-GCAGAGGAAATCGAGCATCCA-3′
TRF2-F: 5′-GTACGGGGACTTCAGACAGAT-3′
TRF2-R: 5′-CGCGACAGACACTGCATAAC-3′

Western blot analysis

Cells were lysed in ice cold RIPA buffer (50mM Tris-HCl, pH 7.4, 150 mM NaCl, 1% NP-40, 0.5% sodium deoxycholate, 0.1% SDS (Sigma)) supplemented with proteinase inhibitors (1 mM PMSF (Roche)). Cell lysates were sonicated at 80% amplitude for 15 s and then cleared by centrifugation at 1000 rpm for 5 minutes. Total protein content was measured for each sample using the BCA assay before 5 × loading buffer (bromophenol blue (0.25%), glycerol (50%), SDS (sodium dodecyl sulfate; 10%), Tris-HCl (0.25 M, pH 6.8), 2-mercaptoethanol (3.6%)) was added and protein samples were boiled for 10 minutes. Equal amounts of protein were loaded and separated on 10% SDS-PAGE gels. Proteins were then transferred onto PVDF membranes (Millipore) using wet transfer with transfer buffer (25 mM Tris base, 189 mM glycine, 20% methanol). Membranes were washed in PBST and blocked with 5% non-fat milk in TBST for 1 hour, followed by sequential incubation with primary and HRP-labeled secondary antibodies. Signals were detected using ImageQuant LAS 4000 from GE Healthcare.

Live imaging

Time-Lapse Imaging. CldU-pulsed cells were plated onto poly-L-lysine-coated 12-well plate in the absence of CldU. After one cell division, cells were synchronized in late G2 phase and release to mitotic phase for photography. In the final step, cells were fixed for CldU staining. Filming of cells was carried out with a Nikon inverted microscope.

Analysis of mitotic defects

Cells were inoculated on poly-L-Lysine coated glass coverslips and grown for 16 h in the absence or in the presence of 0.3 μM APH. For 'chromatin bridges', 'lagging chromosome' and 'micronuclei' analysis, cells were released for additional 1 hour before being fixed with 4% paraformaldehyde for 15 min and permeabilized with 0.5% Triton X-100 in PBS for 20 min. Coverslips were saturated using BSA 3%, Triton X-100 0.5% in PBS for a minimum of 1 hour. Slides were then mounted in mounting medium containing DAPI.

QUANTIFICATION AND STATISTICAL ANALYSIS

GraphPad Prism 6 software was used for statistical analysis, and results were displayed as the means ± SEM. Statistical significance was determined with Student's t tests, one-way Anova or two-way Anova tests, respectively. Data were considered as statistically significant at $p < 0.05$, *$p < 0.05$, **$p < 0.01$, ***$p < 0.001$, ****$p < 0.001$.